Current Research in Microbial Sciences 1 (2020) 1–6

Contents lists available at ScienceDirect

Current Research in Microbial Sciences

journal homepage: www.elsevier.com/locate/crmicr

Imaging living obligate anaerobic bacteria with bilin-binding fluorescent proteins

Hannah E. Chia[a], Tiancheng Zuo[b], Nicole M. Koropatkin[c], E. Neil G. Marsh[b,d], Julie S. Biteen[a,b,*]

[a] Program in Chemical Biology, University of Michigan, Ann Arbor, MI, USA
[b] Department of Chemistry, University of Michigan, Ann Arbor, MI, USA
[c] Department of Microbiology and Immunology, University of Michigan Medical School, Ann Arbor, MI, USA
[d] Department of Biological Chemistry, University of Michigan, Ann Arbor, MI, USA

ARTICLE INFO

Keywords:
Oxgen-independent imaging
Fluorescence microscopy
Microbiome
Fluorogenic ligands

ABSTRACT

Fluorescent tools such as green fluorescent protein (GFP) have been used extensively as reporters in biochemistry and microbiology, but GFP and other conventional fluorescent proteins are restricted to aerobic environments. This limitation precludes fluorescence studies of anaerobic ecologies including polymicrobial communities in the human gut microbiome and in soil microbiomes, which profoundly affect health, disease, and the environment. To address this limitation, we describe the first implementation of two bilin-binding fluorescent proteins (BBFPs), UnaG and IFP2.0, as oxygen-independent fluorescent labels for live-cell imaging in anaerobic bacteria. Expression of UnaG or IFP2.0 in the prevalent gut bacterium *Bacteroides thetaiotaomicron* (*B. theta*) results in detectable fluorescence upon the addition of the bilirubin or biliverdin ligand, even in anaerobic conditions. Furthermore, these BBFPs can be used in two-color imaging to differentiate cells expressing either UnaG or IFP2.0; UnaG and IFP2.0 can also be used to distinguish *B. theta* from other common gut bacterial species in mixed-culture live-cell imaging. BBFPs are promising fluorescent tools for live-cell imaging investigations of otherwise inaccessible anaerobic polymicrobial communities.

Introduction

While green fluorescent protein (GFP) and other genetically encodable fluorescent proteins (FPs) are powerful and ubiquitous tools in biology, these GFP-like FPs are not fluorescent in the absence of oxygen (Tsien, 1998). This oxygen dependence precludes their ability to provide additional insight in anaerobic environments. Many anaerobic systems, like the gut microbiome (Koropatkin et al., 2012; Marchesi et al., 2016) and soil microbiomes (Chaparro et al., 2012; Fierer, 2017), are medically and ecologically important to study, yet remain underexplored because of a lack of appropriate fluorescent probes. Thus, the development of oxygen-independent fluorescent reporters is essential to discover and understand biological and biophysical processes in anaerobic systems.

Previously, fluorescence microscopy studies of anaerobic systems have circumvented the challenges of oxygen-free environments by investigating fixed cells. For example, much of our understanding of the spatial organization of obligate anaerobes comes from imaging of fixed, antibody-stained cells (Earle et al., 2015; Rogers et al., 2013) or cells that express FPs which are exposed to oxygen during fixation (Whitaker et al., 2017). Flavin mononucleotide (FMN) based FPs (FbFPs) are among the few tools that have been demonstrated to label live anaerobic bacteria (Drepper et al., 2007); however, FbFPs are confined to the blue spectral range, which overlaps with intrinsic cellular fluorescence. Despite engineering (Mukherjee et al., 2015; Buckley et al., 2016), FbFP variants also remain dim compared to EGFP. We have previously labeled and studied live anaerobic bacteria with several other probes, but each labeling approach comes with significant limitations (Chia et al., 2019). In one approach, enzymes in the Starch Utilization System (Martens et al., 2009) (Sus) of the prevalent gut bacterium *Bacteroides thetatiotaomicron* (*B. theta*) were tagged with photoactivatable mCherry (PAmCherry) (Tuson et al., 2018). PAmCherry is suitable for single-molecule super-resolution and tracking experiments, but this probe, like GFP, requires oxygen exposure for fluorescence maturation, so measurements of Sus-PAmCherry fusions were done in dormant *B. theta*. On the other hand, we achieved fully anaerobic live-cell imaging by using the HaloTag system to label Sus proteins in single-particle tracking (Karunatilaka et al., 2014). The bright fluorescent dye ligands used in HaloTag systems provide high signal, but significant washing is required to avoid increased background. These ligands are also largely impermeable to bacterial cells and are restricted to outer membrane la-

Abbreviations: BBFP, bilin-binding fluorescent proteins; br, bilirubin; bv, biliverdin; FP, fluorescent protein; GFP, green fluorescent protein.

* Corresponding author at: Department of Chemistry, University of Michigan, Ann Arbor, MI, USA.
E-mail address: jsbiteen@umich.edu (J.S. Biteen).

https://doi.org/10.1016/j.crmicr.2020.04.001
Received 17 March 2020; Received in revised form 16 April 2020; Accepted 16 April 2020

beling without the aid electroporation or osmotic shock (Stagge et al., 2013). These invasive washing and labeling processes prevent in situ HaloTag labeling.

To achieve non-perturbative labeling for investigations of microbial communities, we therefore seek other reporters (Chia et al., 2019). Bilin-binding fluorescent proteins (BBFPs) are particularly attractive options for anaerobic live-cell imaging. BBFPs, such as the green UnaG (Kumagai et al., 2013) and the far-red IFP2.0 (Yu et al., 2014), bind ligands to produce a fluorescent holoprotein rather than relying on an oxidation reaction for chromophore maturation. The ligands bilirubin (br) and biliverdin (bv), bound by UnaG and IFP2.0, respectively, are fluorogenic molecules that produce no background fluorescence even when supplied in excess (Kumagai et al., 2013; Yu et al., 2014). These ligands are cell-permeable in bacteria (Chen et al., 2012), thus allowing labeling of both cytoplasmic and extracellular targets. Both UnaG and IFP2.0 can used in genetically tractable organisms and in most conventional microscopes. UnaG excitation and emission are within the GFP range and UnaG was previously characterized to be approximately as bright as GFP (Kumagai et al., 2013). Although IFP2.0 is dimmer than UnaG or GFP, IFP2.0 emits in the far-red range of visible light (Yu et al., 2014), at wavelengths that suffer from less intrinsic background fluorescence in biological samples.

Here, we implement these two BBFPs, UnaG and IFP2.0, to fluorescently label living *B. theta* cells in the cytoplasm and on the outer membrane. We demonstrate that unlike GFP-labeled *B. theta* cells which only fluoresce in aerobic conditions, UnaG- and IFP2.0-labeled cells fluoresce in live-cell, anaerobic imaging conditions. UnaG-labeled cells can also be used to differentiate *B. theta* from another prevalent gut bacterium, *Ruminococcus bromiii* (*R. bromii*). Furthermore, UnaG-labeled *Bacteroides ovatus* (*B. ovatus*) cells can be distinguished from IFP2.0-labeled *B. theta* cells, indicating that BBFPs can also be used in two-color imaging. Overall, we demonstrate the utility of BBFPs for non-invasive investigations of anaerobic microbial ecologies.

Materials and methods

Bacterial strains cloning and cell cultures

Oligonucleotides and plasmids used in cloning are described in Table S1 plasmids and Table S2 oligonucleotides, respectively. DNA sequencing was used to confirm assembled genes in plasmids.

B. theta and *B. ovatus* strains were generated by counter-selectable allelic exchange in a thymidine kinase deletion (Δ*tdk*) mutant and grown as previously described (Koropatkin et al., 2008). In summary, *B. theta* and *B. ovatus* were first cultured in rich media containing tryptone-yeast extract-glucose and incubated anaerobically at 37 ˚C in a Coy chamber. Cultures were subsequently back-diluted into minimal media with a carbohydrate source (0.05% w/v glucose or maltose). Bilirubin (br, Sigma Aldrich) and biliverdin (bv, Sigma Aldrich) stocks were created in DMSO and added to media as required; final concentrations in media were 25 μM and 2.5 μM for br and bv, respectively.

R. bromii was grown in specialized Ruminococcus (Rum) media (per 50 mL of 2× media): yeast extract (0.25 g), $NaHCO_3$ (0.4 g), L-cysteine (0.1 g), $(NH_4)_2SO_4$ (0.09 g), K_2HPO_4 (0.045 g), KH_2PO_4 (0.045 g), NaCl (0.09 g), $MgSO_4$ (0.004 g), $CaCl_2$ (0.009 g), biotin (20 μg), cobalamin (20 μg), p-aminobenzoic acid (60 μg), folic acid (100 μg), pyridoxamine (300 μg), thiamine (100 μg), riboflavin (100 μg), D-pantothenoic acid hemicalcium salt (100 μg), nicotinamide (100 μg), and resazurin (50 μg). Rum media also contained (concentrations per 50 mL of 2× media): hematin (30 μM), L-histidine (3 mM), acetic acid (63.7 mM), propionic acid (17.8 mM), isobutyric acid (5.75 mM), isovaleric acid (1.95 mM), and valeric acid (1.95 mM). Rum media was diluted with an equal volume of a carbohydrate source (0.05% w/v maltose or fructose and glycogen) to culture cells. Co-cultures were made by growing *R. bromii* anaerobically at 37 ˚C overnight and adding *B. theta* the following day for continued cell growth.

Growth curves

B. theta and *B. ovatus* cells were cultured in minimal media with an appropriate carbohydrate source and back-diluted 1:200 into 96-well clear bottom plates with media. Each growth experiment condition were performed in triplicate. Plates were loaded into a Biostack automated plate-handling device (Biotek Instruments). Absorbance at 600 nm (OD_{600}) was measured in each well every 20 min by a Powerwave HT absorbance reader (Biotek Instruments). Data were recorded using Gen5 software (BioTek Instruments) and Prism (GraphPad).

Fluorescence microscopy

Cells were grown to early to mid-log phase and imaged. All imaging was performed at room temperature and anaerobically on cells sealed between coverslips with epoxy as previously described (Karunatilaka et al., 2013) unless otherwise noted for "+O_2" samples in the figure captions. For immunostaining, *B. theta* cells were incubated with custom rabbit polyclonal SusF antibody (1:100 dilution; Cocalico Biologicals, Inc.) (Tuson et al., 2018) for 30 min and washed with phosphate-buffered saline (PBS) prior to incubation with AlexaFluor 594 secondary anti-rabbit goat antibody (4 μg in 100 μL; ThermoFisher Scientific). Imaging was done in an Olympus IX71 inverted epifluorescence microscope with a 100 × 1.4 N.A. wide-field oil-immersion objective. Samples were illuminated by a 488-nm laser (Coherent Sapphire 488–50; 8–18 W/cm^2), 561-nm laser (Coherent Sapphire 561–50; 120 W/cm^2), or a 640-nm laser (Coherent CUBE 640–40C; 80 W/cm^2). Fluorescence emission was filtered with appropriate filter sets and imaged on a 512 × 512 pixel Photometrics Evolve EMCCD camera at 25 frames/s or on a 512 × 512 pixel Andor iXon EMCCD camera at 100 frames/s. For consistency and noise reduction, final fluorescence images were created by summing frames for a total of 400 ms total integration time. Recorded images and movies were analyzed using ImageJ; all images are presented on the same color scale.

Flow cytometry

Flow cytometry was performed on unlabeled and labeled *B. theta* cells expressing GFP or UnaG with varying concentrations of bilirubin. Cells were analyzed on an Attune NxT Flow Cytometer in the BL1 channel. Data was processed using Attune NxT software.

Protein expression and purification

Like others, we had difficulty expressing the original *UnaG* gene in high enough quantities for successful purification (Yeh et al., 2017). To improve solubility and protein expression, we ordered *UnaG* that was codon-optimized for *E. coli* expression in the vector pMAL-c5x (GenScript) (Sequences S1). The transcribed protein was UnaG with maltose-binding-protein (MBP) on the N-terminus and 6x-His on the C-terminus; the protein herein is referred to as UnaG. UnaG was expressed in *E. coli* (NEB-Express) with IPTG induction (0.4 mM final concentration). Cell pellets were lysed by sonication and after centrifugation, the supernatant was collected and loaded onto affinity columns. UnaG was purified by two rounds of affinity chromatography using fast protein liquid chromatography (Akta Systems): (1) MBP-trap (5 mL, GE Healthcare) and (2) His-trap (5 mL, GE Healthcare). The final elution fractions were dialyzed to remove imidazole and concentrated. For the holoprotein, UnaG was incubated with 2-fold excess ligand (br or bv) and isolated by PD-10 desalting column (5 mL, GE Healthcare).

EGFP was obtained from Addgene (plasmid #54762) and expressed from the pBAD vector in *E. coli* (BL21 DE3) with arabinose induction (0.005% final concentration). Cell pellets were lysed by sonication and purified by nickel column chromatography. Elution fractions were dialyzed to remove imidazole and concentrated.

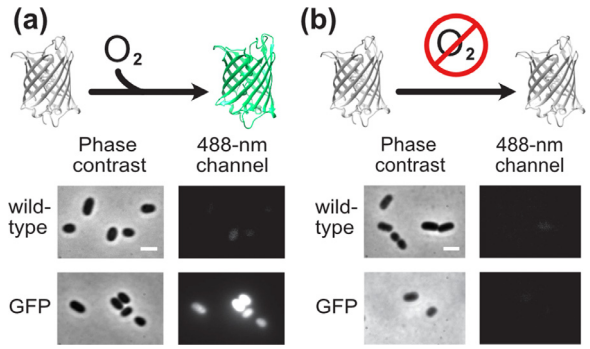

Fig. 1. GFP requires oxygen to produce fluorescence. *B. theta* cells expressing GFP (a) fluoresce in aerobic conditions after 20 min of air exposure and (b) do not fluoresce in anaerobic conditions. Scale bars: 2 μm. PDB ID: 1GFL.

IFP2.0 was obtained from Addgene (plasmid #54785) and inserted into the pBAD vector using Gibson Assembly cloning. IFP2.0 was expressed in *E. coli* (BL21 DE3) with arabinose induction (0.005% final concentration). Cell pellets were lysed by sonication and purified by nickel column chromatography. IFP2.0 was incubated with 2-fold excess ligand (br or bv) and excess ligand was removed by dialysis for 3 h.

Protein characterization

All proteins were prepared for measurements in the same buffer: Tris–HCl (20 mM), NaCl (200 mM), and EDTA (1 mM). UV–Vis absorbance measurements were performed in 96-well clear bottom plates (Molecular Devices SpectraMax iD3 microplate reader). Fluorescence measurements were carried out on an Agilent Varian Cary Eclipse Fluorescence Spectrophotometer. Plotted fluorescence excitation and emission spectra are averaged plots from three technical replicates. Data was processed using MATLAB.

Results and discussion

The use of GFP as a fluorescent tag is restricted to aerobic environments. Though dormant *B. theta* cells labeled with GFP are fluorescent after exposure to oxygen in air (Fig. 1(a)), maintaining the oxygen-free environments for continued cell growth of these anaerobic aerobic cells results in no fluorescence from GFP-labeled *B. theta* cells (Fig. 1(b)).

On the contrary, BBFPs are oxygen-independent fluorescence reporters that bind to a ligand to produce fluorescence (Chia et al., 2019; Kumagai et al., 2013; Yu et al., 2014). UnaG fluoresces only after addition of br (Fig. 2(a)); the purified holoprotein of UnaG with bound br has maximal excitation and emission that is only slightly red-shifted compared to GFP excitation and emission (Fig. 2(b)); UnaG can therefore be imaged with these common microscopy filters. The br ligand is not fluorescent in solution (Figs. 2(c) and (d), S1); this fluorogenic ligand is therefore suitable for supplementing in high concentrations in live-cell imaging without creating background or requiring washing steps. *B. theta* cells expressing codon-optimized UnaG in the cytoplasm and grown with br were fluorescent in both aerobic and anaerobic environments (Fig. 2(c) and (d)). The addition of excess br ligand does not affect the growth kinetics of UnaG-labeled cells (Fig. S2), nor does 25 μM br affect the *B. theta* cell morphology (Fig. S3), thus we selected a br concentration of 25 μM to optimize fluorescent labeling efficiency while minimizing toxicity (Fig. S4).

We implemented IFP2.0 as a second oxygen-independent fluorescence reporter in *B. theta*. Like UnaG, IFP2.0 fluoresces only upon addition of its ligand, bv (Fig. 3(a)), which differs from br in the extent of their conjugated π-systems. The purified holoprotein is maximally excited and emissive in the near-IR range of light (Fig. 3(b), maroon lines). IFP2.0 can also be excited, albeit with a three-fold reduction in emission, at 635-nm (Fig. 3(b), red line), which is the laser wavelength used to excite conventional red dyes like Cy5 and AlexaFluor 633. Like br, the bv ligand has the benefit of being fluorogenic (Figs. 3(c) and (d), S1). *B. theta* cells expressing IFP2.0 grown with bv were fluorescent in both aerobic and anaerobic environments (Fig. 3(c) and (d)), and in fact, we observed that IFP2.0-labeled cells photobleached quickly in aerobic conditions (seconds timescale), whereas IFP2.0-labeled cells did not bleach appreciably on the timescale of anaerobically sealed samples (Figs. 3(c) and (d), S5). The bleaching of IFP2.0-labeled *B. theta* cells in oxygen-exposed conditions may be related to the low photostability of far-red BBFPs (Yu et al., 2015).

The labeled *B. theta* strains in Figs. 2 and 3 constitutively express UnaG or IFP2.0 in the cytoplasm. We also investigated BBFP labeling in fusions to Sus outer-membrane proteins on the *B. theta* surface. We created two *B. theta* strains expressing SusG-UnaG and SusE-IFP2.0, respectively, at the native promoter; we have previously demonstrated that fusions of these proteins to HaloTag and PAmCherry do not disrupt protein function or outer-membrane localization (Tuson et al., 2018). The expression level of the outer membrane fusion proteins was more than 40-fold lower than UnaG or IFP2.0 in cytoplasm expressed FP strains (Whitaker et al., 2017). Fluorescence signal was only weakly detected in the SusG-UnaG strain, possibly because the low copy number of the fusion protein was not enough to overcome signal from intrinsic background fluorescence at this wavelength (Figure S6). On the contrary, though IFP2.0 is dimmer than UnaG (Yu et al., 2014), the intrinsic background fluorescence is reduced at longer wavelengths and SusE-IFP2.0 can still be visualized despite the relatively low copy number (Fig. S6).

To demonstrate the utility of UnaG and IFP2.0 for microscopy of live, anaerobic polymicrobial communities, we imaged these BBFPs in mixed culture. Like *B. theta*, *R. bromii* is another prevalent bacterial species in the human gut microbiome; cross-feeding between these two species is important in establishing a healthy microbial community (Ze et al., 2012). *R. bromii* is not genetically tractable and cannot be fluorescently labeled with genetically encoded tools such as FPs. In phase-contrast mixed cultures of *B. theta* and *R. bromii*, dividing *B. theta* cells are difficult to distinguish from the relatively small and circular *R. bromii* (Fig. 4(a)). However, when mixed cultures of *B. theta* expressing UnaG and *R. bromii* were grown with br, the fluorescent *B. theta* cells (green) were distinguishable from the non-fluorescent *R. bromii* cells (Fig. 4(a)).

Furthermore, two-color imaging can be attained using UnaG and IFP2.0 as a labeling pair. We determined that *B. theta* cells expressing UnaG are fluorescent in the 488-nm channel but not the 635-nm channel whether grown in br or bv. Conversely, *B. theta* cells expressing IFP2.0 are fluorescent in the 635-nm channel but not the 488-nm channel whether grown in br or bv (Fig. S7). This protein specificity was further verified in vitro for purified UnaG and IFP2.0 protein incubated with excess br or bv (Fig. S8). Again, the protein spectrum is independent of the bound ligand. Purified UnaG had a similar fluorescence spectrum when incubated with excess bv or br, albeit with two-fold reduction in emission efficiency in bv. Surprisingly, though IFP2.0-labeled cells grown in br were fluorescent (Fig. S7), we did not measure any fluorescence for purified IFP2.0 incubated with excess br excited at 635 nm; we attribute these differences to the fact that the single-molecule microscope used in these imaging experiments is more sensitive than a fluorescence spectrophotometer (Tuson and Biteen, 2015).

Based on this ability to distinguish UnaG from IFP2.0 regardless of the ligand identity, we imaged a mixed culture of UnaG-labeled *B. ovatus* cells and IFP2.0-labeled *B. theta* cells grown in both br and bv, and differentiated between the two cell strains based on imaging in separate color channels (Fig. 4(b)). Immunofluorescence staining of *B. theta* using polyclonal antibodies against SusF, a *B. theta*-specific protein, was imaged in a third channel to independently identify the *B. theta* cells.

To our knowledge, this work demonstrates the first example of applying BBFPs to live-cell imaging of obligate anaerobic bacteria. The blue-green UnaG and the red IFP2.0 can fluoresce in both aerobic and

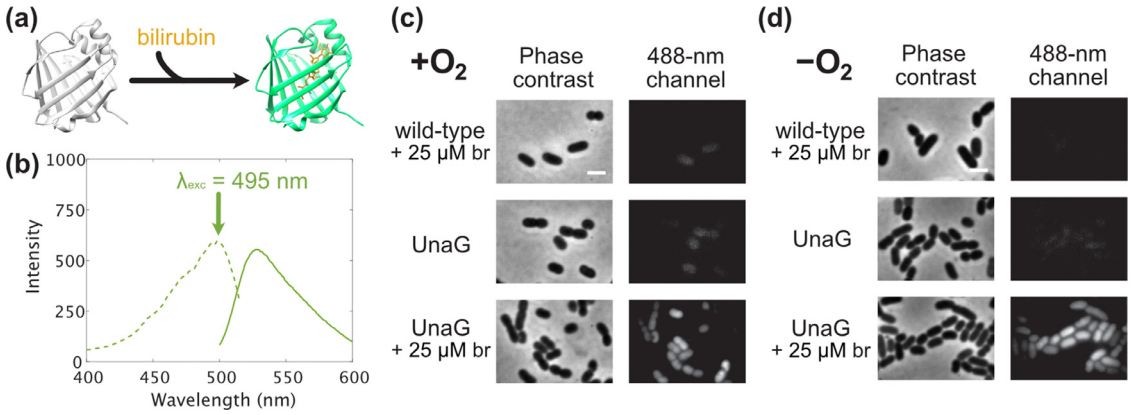

Fig. 2. UnaG uses bilirubin to produce fluorescence. (a) The protein UnaG binds bilirubin (br) to become fluorescent. (b) Purified protein with bound br is maximally excited at 495 nm and has maximal emission at 525 nm. *B. theta* cells expressing UnaG and grown with br fluoresce upon 488-nm excitation in (c) aerobic and (d) anaerobic conditions. Scale bars: 2 μm. PDB ID: 4I3B.

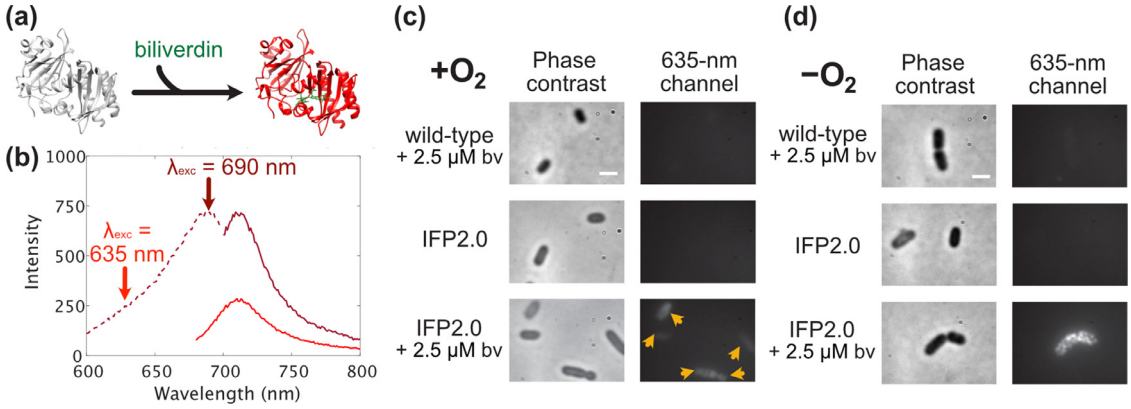

Fig. 3. IFP2.0 uses biliverdin to produce fluorescence. (a) The protein IFP2.0 binds biliverdin (bv) to become fluorescent. (b) Purified protein with bound bv is maximally excited at 690 nm and has maximal emission at 710 nm (burgundy curve). Purified IFP2.0 incubated with bv has reduced emission when excited at 635 nm (red curve). *B. theta* cells expressing IFP2.0 and grown with bv fluoresce upon 635-nm excitation in (c) aerobic and (d) anaerobic conditions. Scale bars: 2 μm. PDB ID: 4CQH.

anaerobic conditions and the wavelength used for fluorescence depends on the protein rather than the ligand bound. Both UnaG and IFP2.0 can fluorescently label *B. theta* in monocultures. In co-cultures, *B. theta* labeled with UnaG can be distinguished from unlabeled *R. bromii*. Finally, UnaG and IFP2.0 labeled cells could be distinguished from one another in two-color imaging.

Among the options for oxygen-independent fluorescent reporters (Chia et al., 2019), BBFPs are an attractive option for further optimization. Flavin-mononucleotide (FMN)-based FPs work in live-cell imaging because the FMN cofactor is readily accessible, but these reporters are confined to the blue spectral region and are weakly fluorescent (Wingen et al., 2014). HaloTag (Los et al., 2008) and other self-labeling tags like SNAP (Keppler et al., 2003) and CLIP (Gautier et al., 2008) specifically bind bright fluorescent dyes but require a wash step to eliminate excess ligand; this treatment may not be compatible with continuous live-cell imaging and may disrupt microbial communities. Recent developments have yielded fluorogenic dyes for HaloTag (Liu et al., 2017; Grimm et al., 2017) and SNAP-tag (Komatsu et al., 2011; Sun et al., 2011; Lukinavičius et al., 2016) that circumvent the need for washing and increase applications in single-molecule imaging. However, these ligands may still suffer from the low cell permeability in bacteria that limits their utility in labeling cytoplasmic targets. In our past experiments using HaloTag technology, we have not successfully labeled bacterial proteins in anaerobes other than targets expressed on the outer membrane (Karunatilaka et al., 2014). It may also be feasible to implement other ligand-dependent reporter systems such as Y-FAST (Plamont et al., 2016), antibody-based fluorogen activating proteins (Szent-Gyorgyi et al., 2008), and engineered fluorogen-dependent proteins (G. Bozhanova et al., 2017; Povarova et al., 2019; Sheng et al., 2018) in anaerobic bacteria using cell-permeable fluorogenic ligands to provide the same advantages of oxygen-independent labeling as BBFPs. Previously, BBFPs have been demonstrated in live-cell mammalian systems (Yu et al., 2014; Yu et al., 2015). In these applications, as in the current paper, br and bv do not lead to undesired background fluorescence; moreover, in mammalian cells br and bv may be endogenously released by heme degradation and interconverted in cells by endogenous oxidoreductases.

IFP2.0 has already been engineered to be a bright and monomeric FP variant from the phytochrome protein family (Yu et al., 2014; Shu et al., 2009). Here, we have shown that IFP2.0 is an appropriate red label for live-cell imaging in anaerobic bacteria. Future developments in the IFP family of FPs will further improve this application. For instance, IFP2.0 dimerizes at high concentrations and was recently further modified to produce mIFP, a monomeric red BBFP (Yu et al., 2015); IFP2.0 aggregation may explain the distinct puncta we observed in the *B. theta* strains with highly expressed IFP2.0 (Fig. 3(d)). Overall, these red-shifted FPs are highly desirable for in vivo imaging with applications in deep tissue imaging and thick biofilms.

While UnaG has recently been demonstrated as a useful tool for single-molecule imaging as a dark-to-green photoswitchable FP (Kwon et al., 2020), this FP has yet to be as extensively optimized as IFP2.0, and it is possible that UnaG can be diversified to a palette of different fluorescent colors. Others engineered UnaG to create a brighter and more stable variant containing a single V2L mutation (Yeh et al.,

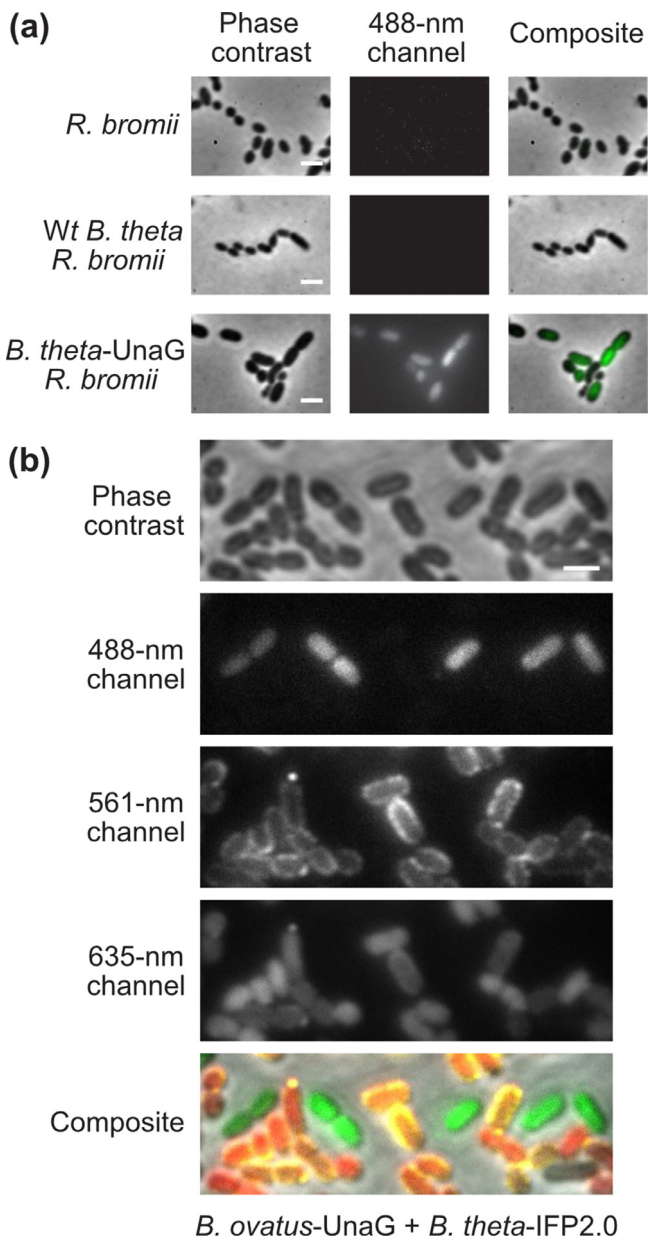

Fig. 4. BBFPs can be used in mixed culture imaging and multi-color imaging. (a) *B. theta* expressing UnaG (green) is distinguished from unlabeled *R. bromii* when grown in mixed culture with br. Scale bars: 2 μm. (b) When grown in media containing br and bv, *B. ovatus* expressing UnaG is differentiated from *B. theta* expressing IFP2.0 in separate color channels using 488-nm (green) and 635-nm (red) excitation, respectively. Immunofluorescence staining imaged at 561 nm independently identified *B. theta* cells. Scale bar: 2 μm. (For interpretation of the references to color in this figure legend, the reader is referred to the web version of this article.)

2017). While no one has attempted to do so, it is possible that UnaG can be diversified to a palette of different fluorescent colors. Since UnaG binds br non-covalently using a hydrophobic pocket, we initially postulated that the protein could accommodate different fluorogenic small molecules as a ligand. We hypothesized that UnaG could bind bv as an alternative ligand and that the extended π-conjugation of bv would red-shift UnaG holoprotein excitation and emission. Others have noted that UnaG does not fluoresce using bv (Kumagai et al., 2013). Similarly, we did not observe any red fluorescence when UnaG was bound to bv instead of br. However, we observed some fluorescence in the original 495/525 nm range, albeit with a diminished intensity (Figs. S7 and S8). These results suggest that may be some spontaneous or endogenous interconversion between br and bv. Likewise, both the BBFP binding pocket and the ligand itself are important factors in determining fluorescence intensity and color.

Conclusions

We have demonstrated that the BBFPs UnaG and IFP2.0 are well-suited probes for anaerobic live-cell imaging. Unlike GFP, both UnaG and IFP2.0 can fluorescently label obligate anaerobic bacteria regardless of oxygen exposure. Furthermore, fluorescence was detectable without perturbing the sample in a washing step. These proteins can be used to label strains in mixed bacterial cultures and can be used for two-color imaging as complementary probes, using common GFP and Cy5 filter cubes. We therefore foresee the use of BBFPs as labels for imaging more complex, polymicrobial communities and in general for studying living biological systems that require oxygen-free environments.

Declaration of Competing Interest

The authors declare that they have no known competing financial interests or personal relationships that could have appeared to influence the work reported in this paper.

Acknowledgments

This work was supported by Army Research Office grant W911NF-18-1-0339 to J.S.B., National Institutes of Health grant GM118475 to N.M.K., and National Institutes of Health grant GM093088 to E.N.G.M.; H.E.C. was also supported by the National Science Foundation Graduate Research Fellowship Program grant DGE-1256260. We thank Laura Buttita for access to the flow cytometer and Eric Martens for access to the plate reader system. We thank Su Chen, Jiawang Zhou, and Michael R. Wasielewski for helpful discussions about fluorescence.

Supplementary materials

Supplementary material associated with this article can be found in the online version at doi:10.1016/j.crmicr.2020.04.001.

References

Bozhanova, N.G., Baranov, M.S., Klementieva, N.V., Sarkisyan, K.S., Gavrikov, A.S., Yampolsky, I.V., Zagaynova, E.V., Lukyanov, S.A., Lukyanov, K.A., Mishin, A.S., 2017. Protein labeling for live cell fluorescence microscopy with a highly photostable renewable signal. Chem. Sci. 8, 7138–7142.

Buckley, A.M., Jukes, C., Candlish, D., Irvine, J.J., Spencer, J., Fagan, R.P., Roe, A.J., Christie, J.M., Fairweather, N.F., Douce, G.R., 2016. Lighting up clostridium difficile: reporting gene expression using fluorescent Lov domains. Sci. Rep. 6, 23463.

Chaparro, J.M., Sheflin, A.M., Manter, D.K., Vivanco, J.M., 2012. Manipulating the soil microbiome to increase soil health and plant fertility. Biol. Fertil. Soils 48, 489–499.

Chen, D., Brown, J.D., Kawasaki, Y., Bommer, J., Takemoto, J.Y., 2012. Scalable production of biliverdin IXα by *Escherichia coli*. BMC Biotechnol. 12, 89.

Chia, H.E., Marsh, E.N.G., Biteen, J.S., 2019. Extending fluorescence microscopy into anaerobic environments. Curr. Opin. Chem. Biol. 51, 98–104.

Drepper, T., Eggert, T., Circolone, F., Heck, A., Krauß, U., Guterl, J.-K., Wendorff, M., Losi, A., Gärtner, W., Jaeger, K.-E., 2007. Reporter proteins for in vivo fluorescence without oxygen. Nat. Biotechnol. 25, 443–445.

Earle, K.A., Billings, G., Sigal, M., Lichtman, J.S., Hansson, G.C., Elias, J.E., Amieva, M.R., Huang, K.C., Sonnenburg, J.L., 2015. Quantitative imaging of gut microbiota spatial organization. Cell Host Microbe 18, 478–488.

Fierer, N., 2017. Embracing the unknown: disentangling the complexities of the soil microbiome. Nat. Rev. Microbiol. 15, 579–590.

Gautier, A., Juillerat, A., Heinis, C., Corrêa Jr., I.R., Kindermann, M., Beaufils, F., Johnsson, K., 2008. An engineered protein tag for multiprotein labeling in living cells. Chem. Biol. 15, 128–136.

Grimm, J.B., Muthusamy, A.K., Liang, Y., Brown, T.A., Lemon, W.C., Patel, R., Lu, R., Macklin, J.J., Keller, P.J., Ji, N., et al., 2017. A general method to fine-tune fluorophores for live-cell and in vivo imaging. Nat. Methods 14, 987–994.

Karunatilaka, K.S., Cameron, E.A., Martens, E.C., Koropatkin, N.M., Biteen, J.S., 2014. Superresolution imaging captures carbohydrate utilization dynamics in human gut symbionts. MBio 5 e02172–e02114.

Karunatilaka K.S., Coupland B.R., Cameron E.A., Martens E.C., Koropatkin N.K., Biteen J.S.: Single-molecule imaging can be achieved in live obligate anaerobic bacteria. 2013:85900K-85900K–7.
Keppler, A., Gendreizig, S., Gronemeyer, T., Pick, H., Vogel, H., Johnsson, K., 2003. A general method for the covalent labeling of fusion proteins with small molecules in vivo. Nat. Biotechnol. 21, 86–89.
Komatsu, T., Johnsson, K., Okuno, H., Bito, H., Inoue, T., Nagano, T., Urano, Y., 2011. Real-time measurements of protein dynamics using fluorescence activation-coupled protein labeling method. J. Am. Chem. Soc. 133, 6745–6751.
Koropatkin, N.M., Cameron, E.A., Martens, E.C., 2012. How glycan metabolism shapes the human gut microbiota. Nat. Rev. Microbiol. 10, 323–335.
Koropatkin, N.M., Martens, E.C., Gordon, J.I., Smith, T.J., 2008. Starch catabolism by a prominent human gut symbiont is directed by the recognition of amylose helices. Structure 16, 1105–1115.
Kumagai, A., Ando, R., Miyatake, H., Greimel, P., Kobayashi, T., Hirabayashi, Y., Shimogori, T., Miyawaki, A., 2013. A bilirubin-inducible fluorescent protein from eel muscle. Cell 153, 1602–1611.
Kwon, J., Park, J.-.S., Kang, M., Choi, S., Park, J., Kim, G.T., Lee, C., Cha, S., Rhee, H.-.W., Shim, S.-.H., 2020. Bright ligand-activatable fluorescent protein for high-quality multicolor live-cell super-resolution microscopy. Nat. Commun. 11, 1–11.
Liu, Y., Miao, K., Dunham, N.P., Liu, H., Fares, M., Boal, A.K., Li, X., Zhang, X., 2017. The cation–π interaction enables a halo-tag fluorogenic probe for fast no-wash live cell imaging and gel-free protein quantification. Biochemistry 56, 1585–1595.
Los, G.V., Encell, L.P., McDougall, M.G., Hartzell, D.D., Karassina, N., Zimprich, C., Wood, M.G., Learish, R., Ohana, R.F., Urh, M., et al., 2008. HaloTag: a novel protein labeling technology for cell imaging and protein analysis. ACS Chem. Biol. 3, 373–382.
Lukinavičius, G., Reymond, L., Umezawa, K., Sallin, O., D'Este, E., Göttfert, F., Ta, H., Hell, S.W., Urano, Y., Johnsson, K., 2016. Fluorogenic probes for multicolor imaging in living cells. J. Am. Chem. Soc. 138, 9365–9368.
Marchesi, J.R., Adams, D.H., Fava, F., Hermes, G.D.A., Hirschfield, G.M., Hold, G., Quraishi, M.N., Kinross, J., Smidt, H., Tuohy, K.M., et al., 2016. The gut microbiota and host health: a new clinical frontier. Gut 65, 330–339.
Martens, E.C., Koropatkin, N.M., Smith, T.J., Gordon, J.I., 2009. Complex glycan catabolism by the human gut microbiota: the bacteroidetes sus-like paradigm. J. Biol. Chem. 284, 24673–24677.
Mukherjee, A., Weyant, K.B., Agrawal, U., Walker, J., Cann, I.K.O., Schroeder, C.M., 2015. Engineering and characterization of new LOV-based fluorescent proteins from chlamydomonas reinhardtii and vaucheria frigida. ACS Synth. Biol. 4, 371–377.
Plamont, M.-.A., Billon-Denis, E., Maurin, S., Gauron, C., Pimenta, F.M., Specht, C.G., Shi, J., Quérard, J., Pan, B., Rossignol, J., et al., 2016. Small fluorescence-activating and absorption-shifting tag for tunable protein imaging in vivo. Proc. Natl. Acad. Sci. 113, 497–502.
Povarova, N.V., Zaitseva, S.O., Baleeva, N.S., Smirnov, A.Yu., Myasnyanko, I.N., Zagudaylova, M.B., Bozhanova, N.G., Gorbachev, D.A., Malyshevskaya, K.K., Gavrikov, A.S., et al., 2019. Red-shifted substrates for FAST fluorogen-activating protein based on the GFP-like chromophores. Chem. – Eur. J. 25, 9592–9596.
Rogers, T.E., Pudlo, N.A., Koropatkin, N.M., Bell, J.S.K., Balasch, M.M., Jasker, K., Martens, E.C., 2013. Dynamic responses of Bacteroides thetaiotaomicron during growth on glycan mixtures. Mol. Microbiol. 88, 876–890.
Sheng, W., Nick, S.T., Santos, E.M., Ding, X., Zhang, J., Vasileiou, C., Geiger, J.H., Borhan, B., 2018. A near-infrared photoswitchable protein–fluorophore tag for no-wash live cell imaging. Angew. Chem. Int. Ed. 57, 16083–16087.
Shu, X., Royant, A., Lin, M.Z., Aguilera, T.A., Lev-Ram, V., Steinbach, P.A., Tsien, R.Y., 2009. Mammalian expression of infrared fluorescent proteins engineered from a bacterial phytochrome. Science 324, 804–807.
Stagge, F., Mitronova, G.Y., Belov, V.N., Wurm, C.A., Jakobs, S., 2013. Snap-, CLIP- and halo-tag labelling of budding yeast cells. PLoS ONE 8, e78745.
Sun, X., Zhang, A., Baker, B., Sun, L., Howard, A., Buswell, J., Maurel, D., Masharina, A., Johnsson, K., Noren, C.J., et al., 2011. Development of SNAP-Tag Fluorogenic Probes for Wash-free fluorescence imaging. ChemBioChem 12, 2217–2226.
Szent-Gyorgyi, C., Schmidt, B.F., Creeger, Y., Fisher, G.W., Zakel, K.L., Adler, S., Fitzpatrick, J.A.J., Woolford, C.A., Yan, Q., Vasilev, K.V., et al., 2008. Fluorogen-activating single-chain antibodies for imaging cell surface proteins. Nat. Biotechnol. 26, 235–240.
Tsien, R.Y., 1998. The green fluorescent protein. Annu. Rev. Biochem. 67, 509–544.
Tuson, H.H., Biteen, J.S., 2015. Unveiling the inner workings of live bacteria using super-resolution microscopy. Anal. Chem. 87, 42–63.
Tuson, H.H., Foley, M.H., Koropatkin, N.M., Biteen, J.S., 2018. The starch utilization system assembles around stationary starch-binding proteins. Biophys. J. 115, 242–250.
Whitaker, W.R., Shepherd, E.S., Sonnenburg, J.L., 2017. Tunable expression tools enable single-cell strain distinction in the gut microbiome. Cell 169, 538–546.e12.
Wingen, M., Potzkei, J., Endres, S., Casini, G., Rupprecht, C., Fahlke, C., Krauss, U., Jaeger, K.-.E., Drepper, T., Gensch, T., 2014. The photophysics of LOV-based fluorescent proteins – new tools for cell biology. Photochem. Photobiol. Sci. 13, 875–883.
Yeh, J.T.-H., Nam, K., Yeh, J.T.-H., Perrimon, N., 2017. eUnaG: a new ligand-inducible fluorescent reporter to detect drug transporter activity in live cells. Sci. Rep. 7, 41619.
Yu, D., Baird, M.A., Allen, J.R., Howe, E.S., Klassen, M.P., Reade, A., Makhijani, K., Song, Y., Liu, S., Murthy, Z., et al., 2015. A naturally monomeric infrared fluorescent protein for protein labeling in vivo. Nat. Methods 12, 763–765.
Yu, D., Gustafson, W.C., Han, C., Lafaye, C., Noirclerc-Savoye, M., Ge, W.-.P., Thayer, D.A., Huang, H., Kornberg, T.B., Royant, A., et al., 2014. An improved monomeric infrared fluorescent protein for neuronal and tumour brain imaging. Nat. Commun. 5, 3626.
Ze, X., Duncan, S.H., Louis, P., Flint, H.J., 2012. Ruminococcus bromii is a keystone species for the degradation of resistant starch in the human colon. ISME J. 6, 1535–1543.